

Mesocrystals – Applications and potential

Ming-Guo Ma ^{a,b}, Helmut Cölfen ^{a,*}

^a Department of Chemistry, Physical Chemistry, University of Konstanz, 78457 Konstanz, Germany

^b College of Materials Science and Technology, Beijing Forestry University, Beijing 100083, PR China

A B S T R A C T

Mesocrystals are superstructures of nanoparticles with mutual order and can be intermediates in a non classical particle mediated crystallization reaction. Mesocrystals have various potential applications as functional materials due to their unique combination of nanoparticle properties and order combined with a microscopic or even macroscopic size. They can also show collective and emergent properties. In the past, most attention has been paid to the synthesis and the formation mechanism of mesocrystals and in some cases properties and potential applications were reported. Only recently, the number of studies on mesocrystal applications has increased with a clear focus on photocatalysis, Li ion battery and electrode applications. In this opinion paper, the remarkable progress in the field of mesocrystal applications of the last three years is highlighted including examples, where mesocrystals already now can by far outperform traditional materials with their excellent material properties, which can even reach the theoretically maximally possible value. The future application potential of mesocrystals is also discussed.

Keywords:

Mesocrystal
Non-classical crystallization
Nanoparticle
Energy conversion
Photocatalysis
Lithium ion battery

1. Introduction

Mesocrystals, an abbreviation for mesoscopically structured crystals, are highly ordered nanoparticle superstructures, which show organization of nanocrystals in a crystallographic register [1–7]. It is important to emphasize again, that mesocrystal is a definition for a structure and not a formation mechanism [3,4], although many mesocrystals are formed by self-assembly of nanoparticles. Mesocrystals were defined about 10 years ago and since then received rapidly increasing interest due to their unique combination of nanoparticle properties and order with micro/macrosopic size allowing for collective and emergent properties. Therefore, it is not surprising that mesocrystals have been reported for not only a large number of different crystals including metals, metal oxides, carbonates, and phosphates but also organic crystals like amino acids as discussed in several review papers and a book [1–7]. It is interesting to note that mesocrystals were also found in several biominerals including nacre, sea urchins, corals or egg shells [8,9], which show, that this structure obviously has advantages over other crystal structures and is thus evolutionary favored.

Several mesocrystal formation mechanisms have been published including nanoparticle ordering along an ordered organic matrix, by physical fields and directed interactions, and in mineral bridges connecting two nanoparticles or by other spatial constraints [3,5]. Compared to traditional single crystals and polycrystalline materials, mesocrystals can

have special features and properties including unusual mechanical properties, high specific surface area, improved magnetic and electrochemical performance or directional optical properties, due to nanoparticle size and anisotropic shape, order and mesocrystal porosity. These properties offer new chances for potential applications. In the last three years, remarkable progress was reported on mesocrystal applications. Potential applications as photocatalysts and lithium ion batteries and electrodes have been widely explored with a special focus on TiO₂ mesocrystals.

This opinion paper gives an overview of the application potential of mesocrystals. Various applications of mesocrystals including photocatalysis, lithium ion batteries and electrodes, sensors or optoelectronic and biomedical applications are discussed. Finally, a perspective of the potential for future applications is given.

2. Application potential of mesocrystals

2.1. Photocatalysis

For photocatalytic applications, a mesocrystal structure of the catalyst is advantageous due to a high inner surface area and porosity as well as particle orientation and exposure of catalytically active crystal faces. TiO₂ is a prevailing semiconductor photocatalyst and has received considerable attention. In comparison with traditional commercial P25 TiO₂, TiO₂ mesocrystals could be used for efficient photocatalysis due to their advantageous characteristics such as good crystallinity, high surface area, and sufficient porosity coupled with particle sizes in the

* Corresponding author.

E-mail address: helmut.coelfen@uni-konstanz.de (H. Cölfen).

micrometer range, which allows much easier handling and separation as compared to TiO₂ nanoparticles.

Tartaj and Amarilla prepared porous anatase mesocrystals with 25 nm nanoparticles by the methodology of thermally driven self assembly of inverse micelles and seeded assisted hydrolysis of precursors [10^{**}]. It was shown that these porous mesocrystals exhibited good capabilities for photocatalytic degradation of 2,4 dichlorophenol under UV irradiation, better than the commercial nanoparticle reference sample P25. The authors suggested that the high surface area (290 m² g⁻¹) and good crystallinity led to the good photodegradation capability. Moreover, these mesocrystals also displayed good electrochemical performance and active surfaces for enzyme immobilization (650 mg g⁻¹ substrate). Subsequently, Tartaj produced mesocrystals from <100 nm anatase TiO₂ nanoparticles with adequate photocatalytic properties and good capabilities for enzyme immobilization via a two stage temperature program by the addition of nanoseeds to inverse microemulsions [11]. It is expected that these anatase TiO₂ mesocrystals could be used for multiple applications such as photocatalysis, photoeradication of malignancy, photodynamic therapy, and energy storage devices.

TiO₂ mesocrystalline hexagonal microrods were prepared through self directed assembly within intermediate scaffolds via a thermal method [12^{*}]. The TiO₂ microrods exhibited a superior photocatalytic capacity as compared to TiO₂ polycrystalline nanoparticles (Degussa P25 benchmark). Under identical conditions, the short circuit photocurrent intensity, the amount of photogenerated •OH radicals and the bisphenol A degradation efficiency were approximately 3, 2, and 2.5 times, respectively, higher than those of the Degussa P25 benchmark. The good photocatalytic performance of the TiO₂ mesocrystalline microrods is the result of their high crystallinity, large porosity and oriented subunit alignment as well as exposed high energy {001} facets. Also, a controllable approach combining solid-solid topotactic transformation of NH₄TiOF₃ to anatase TiO₂ and a simple sintering process were applied to prepare anatase TiO₂ mesocrystals with largely exposed {001} facets [13]. The sintering temperature was found to have a remarkable effect on the exposed {001} facets. Temperatures below 700 °C led to unexposed {001} facets, while temperatures above 900 °C led to a mixed

phase of anatase and rutile. The photocatalytic activity of the TiO₂ mesocrystals is much higher than that of the corresponding TiO₂ polycrystalline materials and comparable with that of commercially available P25. The exposed {001} facets are also believed to play a very important role in the photocatalysis process.

A kinetically controlled crystallization process based on a non-aqueous sol-gel synthesis method was used to fabricate recrystallized anatase TiO₂ mesocrystals with a truncated bipyramidal Wulff shape [14]. The material exhibited very good photocatalytic activity with a corresponding half life of 140 min for Rhodamine B degradation under visible light irradiation due to the combination of high crystallinity and high surface area of the recrystallized mesocrystal, compared with 310 min for TiO₂ P25 as a benchmark material. More recently, anatase TiO₂ hierarchical architectures, such as flower-like assemblies composed of leaf-like sheets and spindle-shaped assemblies exposing (101) facets, were synthesized via a template-free approach combined with calcination [15]. It was shown that acetic acid and the original concentration of titanium isopropoxide play crucial roles in the architectures of the obtained assemblies. The photocatalytic activities were evaluated by hydrogen production under ultraviolet irradiation in the absence of molecular oxygen, and the flower-like assemblies exhibited the highest photocatalytic activity, compared with those of the TiO₂ nanoparticles and spindle-shaped mesocrystal assemblies. The enhanced photocatalytic activities could be attributed to the synergetic effect of the architecture, high crystallinity, and the large surface areas of anatase TiO₂. The flower-like assemblies show the largest surface area of 175 m² g⁻¹, compared with 106 m² g⁻¹ and 81 m² g⁻¹ for spindle-shaped mesocrystal assemblies and TiO₂ nanoparticles, respectively.

Besides the pure TiO₂ mesocrystals, TiO₂ mesocrystal nanocomposites containing a second kind of nanoparticle as dopant were also employed as efficient catalysts and are a very interesting hybrid system with better catalytic properties compared to the TiO₂ mesocrystals. For example, novel nanocomposites containing plate-like anatase TiO₂ nanocrystal superstructures and noble metal (Au, Pt) nanoparticles were synthesized by preferentially photodepositing metal nanoparticles on the edge of TiO₂ mesocrystals [16^{**}]. A number of fluorescence bursts with signals above the background level (Fig. 1c) were observed during photoirradiation by

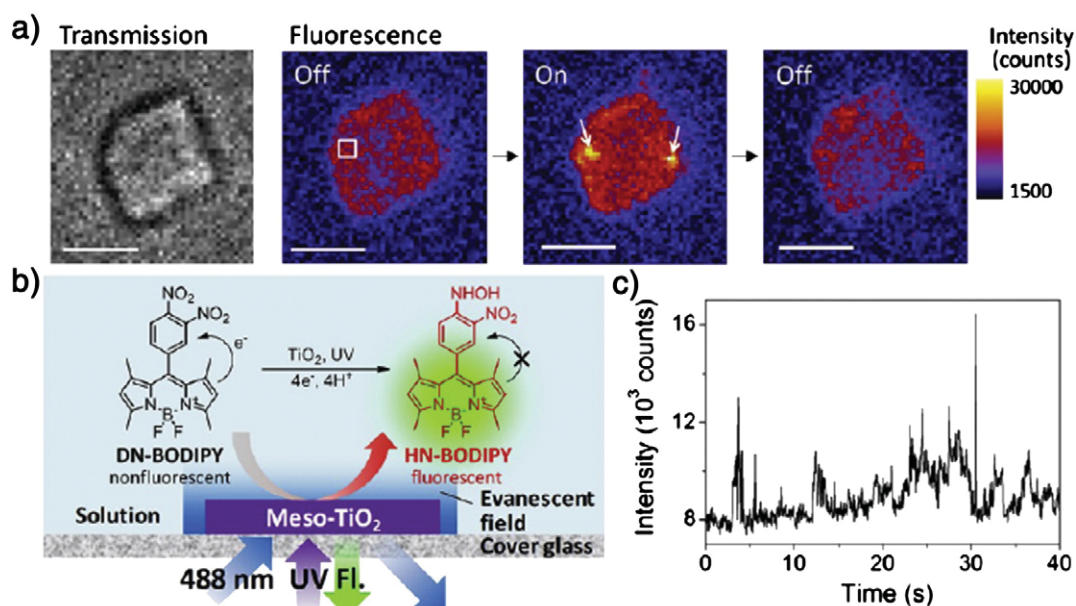


Fig. 1. (a) Optical transmission of an Au/Meso-TiO₂ particle immobilized on a cover glass and fluorescence images of the same particle in Ar-saturated DN-BODIPY solution (0.5 mM in methanol) under 488 nm laser ($I_{488} = 0.1 \text{ kW cm}^{-2}$) and UV irradiation ($I_{UV} = 30 \text{ mW cm}^{-2}$). The fluorescence images display a series of successive images exhibiting on and off events (acquisition time, 50 ms). The arrows point out the location of fluorescence bursts. (b) Single-molecule fluorescence observation by TIRF microscopy and photocatalytic generation of fluorescent HN-BODIPY from non-fluorescent DN-BODIPY. (c) A typical profile of fluorescence intensity obtained from the white box marked in the fluorescence image (panel a). The scale bar is 2 μm .

From Ref. [16^{**}]. Reprinted with permission from ACS.

means of total internal reflection fluorescence (TIRF) microscopy captured for an Au/TiO₂ mesocrystal in Ar saturated methanol containing a probe molecule (3,4 dinitrophenyl BODIPY, DN BODIPY) under both 488 nm laser and UV light irradiation (see Fig. 1a).

Single molecule photocatalytic reduction of DN BODIPY over individual TiO₂ mesocrystals observed by means of TIRF microscopy was used to demonstrate the interfacial electron transfer process on the surface of Meso TiO₂ (see Fig. 1b). Single molecule fluorescence spectroscopy measurements on a single particle directly revealed that most of the photogenerated electrons could migrate from the dominant surface to the edge of the TiO₂ mesocrystal with the reduction reactions mainly occurring at its lateral surfaces containing {101} facets. The loading of metal nanoparticles on the superstructure of TiO₂ was found to greatly improve the photogenerated charge separation efficiency allowing significant (more than 1 order of magnitude) enhancement of the photocatalytic reaction rate in organic degradation reactions as compared to TiO₂ mesocrystals without the noble metal nanoparticles.

Spindle shaped graphene TiO₂ mesocrystal composites were synthesized by a facile template free process based on the combination of sol gel and solvothermal methods [17]. The amount of graphene oxide was found to be of significant influence on the morphologies of TiO₂ mesocrystals and photocatalytic activities of the nanocomposites. Visible light photocatalytic performance of graphene spindle shaped TiO₂ mesocrystal composites indicated that the composites exhibited higher photocatalytic activity than pure TiO₂ mesocrystals and P25, by photocatalytic degradation of Rhodamine B.

However, there is also a report on TiO₂ nanocrystals derived from calcination, which showed superior photocatalytic performance, in comparison to TiO₂ mesocrystals, due to the much higher specific surface area [18]. F127 Pluronic polyethylene oxide (PEO)/polypropylene oxide (PPO) triblock copolymer was used as an additive to effectively obstruct mesoscale assembly of NH₄TiOF₃ nanoparticles and consequently direct the formation of NH₄TiOF₃ mesocrystals. The temperature and the concentration of F127 were found to play an important role in the formation of NH₄TiOF₃ mesocrystals. This function is optimized at a surfactant concentration of 10%. Below this concentration, the low surface coverage of F127 gives rise to aggregation of submicron particles. Above this concentration, however, the hydrophobicity of the PPO chains dominates and induces mesoscale assembly of NH₄TiOF₃ nanoparticles and thereby the formation of NH₄TiOF₃ mesocrystals. Sterically stabilized nanoparticles prepared at 23 °C with 10% of F127 give rise to TiO₂ nanocrystals, whereas NH₄TiOF₃ mesocrystals prepared at 23 °C with 15% of F127 give rise to TiO₂ mesocrystals after calcination at 700 °C.

As a well known wide band gap semiconductor, ZnO mesocrystals have also potential applications as a photocatalyst. A room temperature ionic liquid based process was used for the ultrafast formation of ZnO mesocrystals by using urea and choline chloride as the solvent, and Tris containing deionized water as the anti solvent at 70 °C [19]. ZnO mesocrystals with relatively high specific surface areas (43 m² g⁻¹) showed excellent photocatalytic activities toward photodegradation of methylene blue that was comparable to that of P25 TiO₂. Also, a simple wet chemical procedure was developed for the preparation of rod like ZnO mesocrystals by annealing rod like Zn(OH)₂ tartaric acid composites in air at elevated temperatures. The composites were obtained by simply mixing the aqueous solutions of zinc acetate, sodium hydroxide, and tartaric acid [20]. In comparison with the individual ZnO nanoparticles, the ZnO mesocrystals showed similar photocatalytic performance for the photodegradation of methyl orange and the photoreduction of Cr⁶⁺.

Unlike ZnO mesocrystals, CuO mesocrystals are a p type semiconductor with a narrow band gap, which have potential applications as a photocatalyst. The ordered aggregation driven growth from surfactant free one dimensional (1D) CuO nanocrystals into dimension controlled mesostructures (three dimensional (3D) mesocrystal spindles and two dimensional (2D) mesocrystal plates) was realized by an additive free complex precursor solution route [21]. The reactant concentration was found to affect the products at higher reaction temperature. 3D "layer

by layer" growth of mesostructured CuO spindles was successfully achieved at low reactant concentrations, while the 2D "shoulder by shoulder" growth of mesostructured CuO plates was obtained at high reactant concentrations. The CuO mesocrystal spindles exhibit a higher adsorption and photocatalytic degradation (72.5%) of Rhodamine B than that of 2D CuO mesocrystal plates (51.9%). CuO mesocrystals could serve as a potential photocatalyst for the degradation of Rhodamine B under visible light irradiation in the presence of hydrogen peroxide (H₂O₂).

There have been a few reports on perovskite mesocrystals with potential applications as a photocatalyst. A simple molten salt process was employed for the synthesis of strontium sodium tantalite mesocrystals built from nanocubes (20–60 nm) via a non classical crystallization process [22]. The weight ratio of salt to starting materials was found to influence mesocrystal formation. The strontium sodium tantalite mesocrystals exhibit an outstanding photocatalytic performance due to their nanosteps, high porosity and preferred orientation of their building units as demonstrated for photocatalytic water splitting. Rates of hydrogen generation reach values of 27.5 mmol h⁻¹ for aqueous methanol and 4.89 mmol h⁻¹ for pure water splitting.

A special porous SrTiO₃ 3D mesocrystal architecture was formed by a facile hydrothermal reaction at 150 °C using layered protonated titanate hierarchical spheres of submicrometer size as a precursor template [23]. The mesocrystal was formed through assembly of hundreds of highly oriented nanocubes of 60–80 nm by partial sharing of (100) faces. Compared to the solid SrTiO₃ photocatalysts previously synthesized by high temperature solid state methods, the porous SrTiO₃ mesocrystals had relatively high specific surface areas (up to 21 m² g⁻¹) and exhibited enhanced photocatalytic activity in hydrogen evolution from water splitting.

2.2. Lithium ion batteries & electrode application potential

Mesocrystals can also be used as electrode materials, especially in lithium ion batteries. For this application, a high specific surface area and a high crystallinity of the mesocrystals are also important. As mentioned above, TiO₂ mesocrystals can not only be used in photocatalysis due to their good photocatalytic properties, but can also be applied in energy storage devices thanks to their good electrochemical performance [10].

Wei and co workers developed a low temperature additive free synthetic route for the fabrication of unique nanorod shaped mesocrystals with lengths of about 300 nm and diameter of 60–80 nm through homoepitaxial aggregation of ultrathin rutile TiO₂ nanowires via face to face oriented attachment, accompanied and promoted by a simultaneous phase transformation from precursor hydrogen titanate to rutile TiO₂ [24]. The cycling behavior of an electrochemical cell indicated that the rutile TiO₂ mesocrystals had an excellent performance up to 100 cycles at a current rate of 1 C with a retained reversible capacity of 171 mA h g⁻¹, and had a reversible capacity of ~200 mA h g⁻¹ after 10 cycles at 0.5 C and retained a capacity of ~100 mA h g⁻¹ at a current rate of 5 C, demonstrating a large reversible charge discharge capacity and excellent cycling stability. The high performance could again be attributed to the TiO₂ mesostructure constructed from ultrathin nanowires offering large specific surface area for an intercalation reaction and easy mass and charge transport, as well as sufficient void space accommodating volume change.

Sodium dodecyl benzene sulfonate (SDBS) can be employed as additive for the formation of Wulff shaped and nanorod like porous mesocrystals constructed by ultrathin rutile TiO₂ nanowires through the homoepitaxial self assembly of nanocrystallites [25]. SDBS was found to play a key role in the homoepitaxial self assembly process and the titanate/SDBS ratio determined the octahedral Wulff shape and the nanorod shape. Both types of rutile TiO₂ mesocrystals were applied as electrode materials in rechargeable lithium ion batteries with a large reversible charge discharge capacity, excellent cycling stability and

high rate performance as a result of the high surface area (approximately $90 \text{ m}^2 \text{ g}^{-1}$ for nanorod and $36 \text{ m}^2 \text{ g}^{-1}$ for Wulff shape), as well as sufficient void space.

Dumbbell shaped rutile TiO_2 and nanorod like rutile mesocrystals constructed from ultrathin nanowires, and quasi octahedral anatase TiO_2 mesocrystals built from tiny nanoparticle subunits were synthesized by the use of different counterions in the synthesis [26]. It was suggested that the steric blocking effect of the counterions has a great impact on the arrangement of the TiO_6 octahedra in the titanate precursor, leading to the formation of distinct TiO_2 superstructures with different morphologies and crystalline phases. The TiO_2 superstructures were used as anode materials in lithium ion batteries, and exhibited higher capacity and improved rate performance for lithium ion intercalation compared to commercial anatase TiO_2 nanoparticles with a similar surface area ($200 \text{ m}^2 \text{ g}^{-1}$), due to the intrinsic characteristics of the TiO_2 mesocrystals.

In Qi's work, spindle shaped nanoporous anatase TiO_2 mesocrystals with tunable sizes were synthesized on a large scale using a tetrabutyl titanate-acetic acid system under solvothermal conditions [27]. Acetic acid molecules were found to play multiple key roles during the non-hydrolytic processing of the [001] oriented, highly crystalline anatase mesocrystals. These anatase mesocrystals exhibited remarkable crystalline phase stability and improved performance as anode materials for lithium ion batteries. The specific discharge capacities of anatase mesocrystals were 165 mA h g^{-1} and 152 mA h g^{-1} at 1 and 2 C respectively. High crystallinity combined with high porosity of the nanoporous mesocrystals can be seen as the reason for the facile electron conduction and fast lithium ion transport.

Ti based materials have been intensively investigated and considered as good potential negative electrode materials for lithium ion batteries due to their high safety, superior rate capability and excellent cyclic stability. Hong and Wei summarized the recent progress of a

new class of layered titanate nanostructures and their derivatives, including TiO_2 polymorphs and novel titanate nanostructures of $\text{Zn}_2\text{Ti}_3\text{O}_8$, $\text{Li}_2\text{MTi}_3\text{O}_8$ ($M = \text{Co, Zn, Mg}$) and $\text{Li}_4\text{Ti}_5\text{O}_{12}$, as high performance negative electrode materials for lithium ion batteries [28].

More recently, a kinetically controlled growth strategy was applied to synthesize aligned nanorod arrays of [001] oriented mesocrystalline SnO_2 with four {110} lateral facets on Ti foil in a ternary solvent system comprising acetic acid, ethanol, and water [29**] (see Fig. 2). It was found that this mesocrystalline SnO_2 could be used as anode material for lithium ion batteries with an excellent rate performance showing an initial Coulombic efficiency of 65.6% and a very high reversible capacity of 720 mA h g^{-1} at a current rate of 10 C (namely, 7820 mA g^{-1}) (see Fig. 2).

This reversible capacity is at least a factor of 5 higher compared to commercial Li ion batteries, namely LiCoO_2 (140 mA h g^{-1}); $\text{Li}_2\text{Mn}_2\text{O}_4$ (100 mA h g^{-1}); LiFeO_4 (100 mA h g^{-1}) and $\text{Li}_2\text{FePO}_4\text{F}$ (115 mA h g^{-1}). The theoretical capacity of SnO_2 is $\sim 782 \text{ mA h g}^{-1}$. Therefore, the capacity of the SnO_2 mesocrystal based battery is very close to the theoretically possible capacity, which underlines the exceptional performance of the mesocrystal anode.

A striking example was also reported for the synthesis of leaf like CuO mesocrystals via the oriented attachment mechanism by an electrochemical approach [30*]. The electrical field was found to play an important role in the assembly of nanoparticles. It is reported that this material exhibits a high initial discharge capacity of 1063 mA h g^{-1} , a reversible capacity of 674 mA h g^{-1} , which is close to the theoretical capacity, and a slow capacity fading. A stable capacity above 500 mA h g^{-1} was achieved over 30 cycles, demonstrating the advantage of the CuO mesocrystal structure as anode material for lithium ion batteries.

A biomolecule assisted hydrothermal strategy was used for the synthesis of two dimensional ultra thin $\alpha\text{-Co(OH)}_2$ mesocrystal

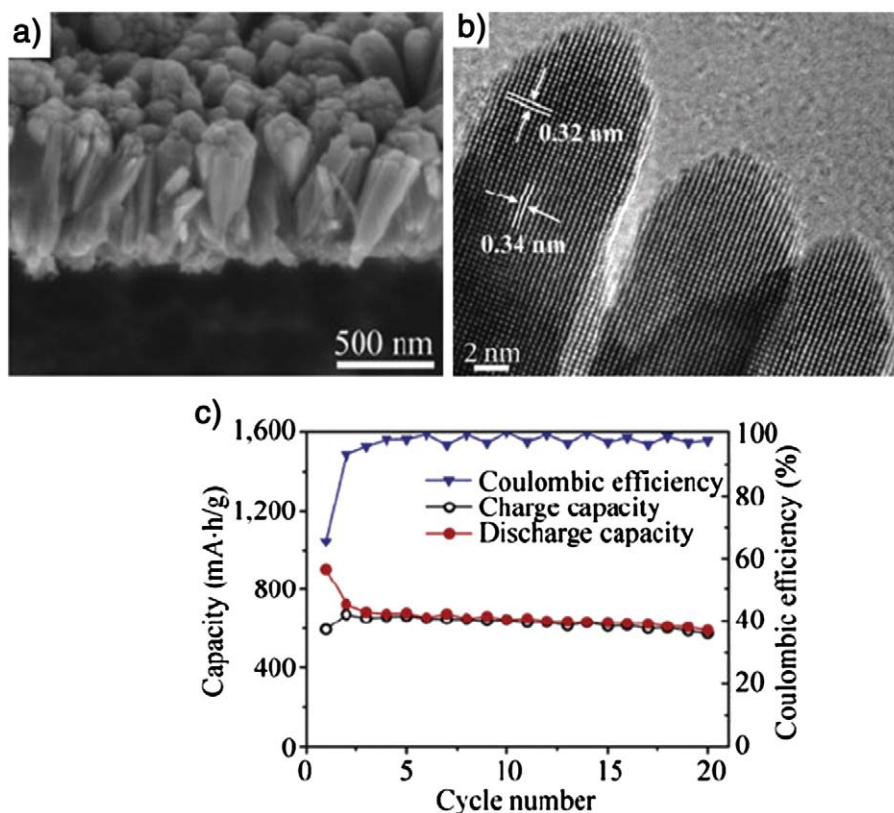


Fig. 2. SEM image (a) and HRTEM image (b), and charge/discharge capacity and Coulombic efficiency (c) of mesocrystalline SnO_2 nanorods. From Ref. [29**]. Reprinted with permission from Springer.

nanosheets [31]. A specific capacitance of 506 F g^{-1} can be achieved by the nanoporous $\alpha\text{-Co(OH)}_2$ mesocrystals at 10 mA cm^{-2} (ca. 1.33 A g^{-1}), and even 427 F g^{-1} at 40 mA cm^{-2} (ca. 5.33 A g^{-1}), revealing their good electrochemical stability at high rates. These mesocrystal nanosheets showed good electrical conductivity, which is highly attractive for application in electrochemical capacitors and Li ion batteries.

A family of hierarchical Li-Mn-O mesocrystals such as LiMn_2O_4 , Li_2MnO_3 , and LiMnO_2 - Li_2MnO_3 consisting of oriented nanocrystals was selectively produced under hydrothermal conditions via a Mn_5O_8 intermediate [32]. The crystal phases could be adjusted by the molar

ratio of LiOH - Mn_5O_8 . The LiMn_2O_4 mesocrystals exhibit better performance (98.2 mA h g^{-1}) than nanoporous particles, which is attributed to the high crystallinity of the faceted mesocrystal. This capacity is in the ballpark of commercial Li ion batteries. Thus, these Li-Mn-O mesocrystals already have considerable potential as electrodes for Li ion batteries.

2.3. Gas sensor applications

Gas sensors are used to detect specific gases including CO , NO_2 , Freon, formaldehyde, ethanol, human oral halitosis, and so on.

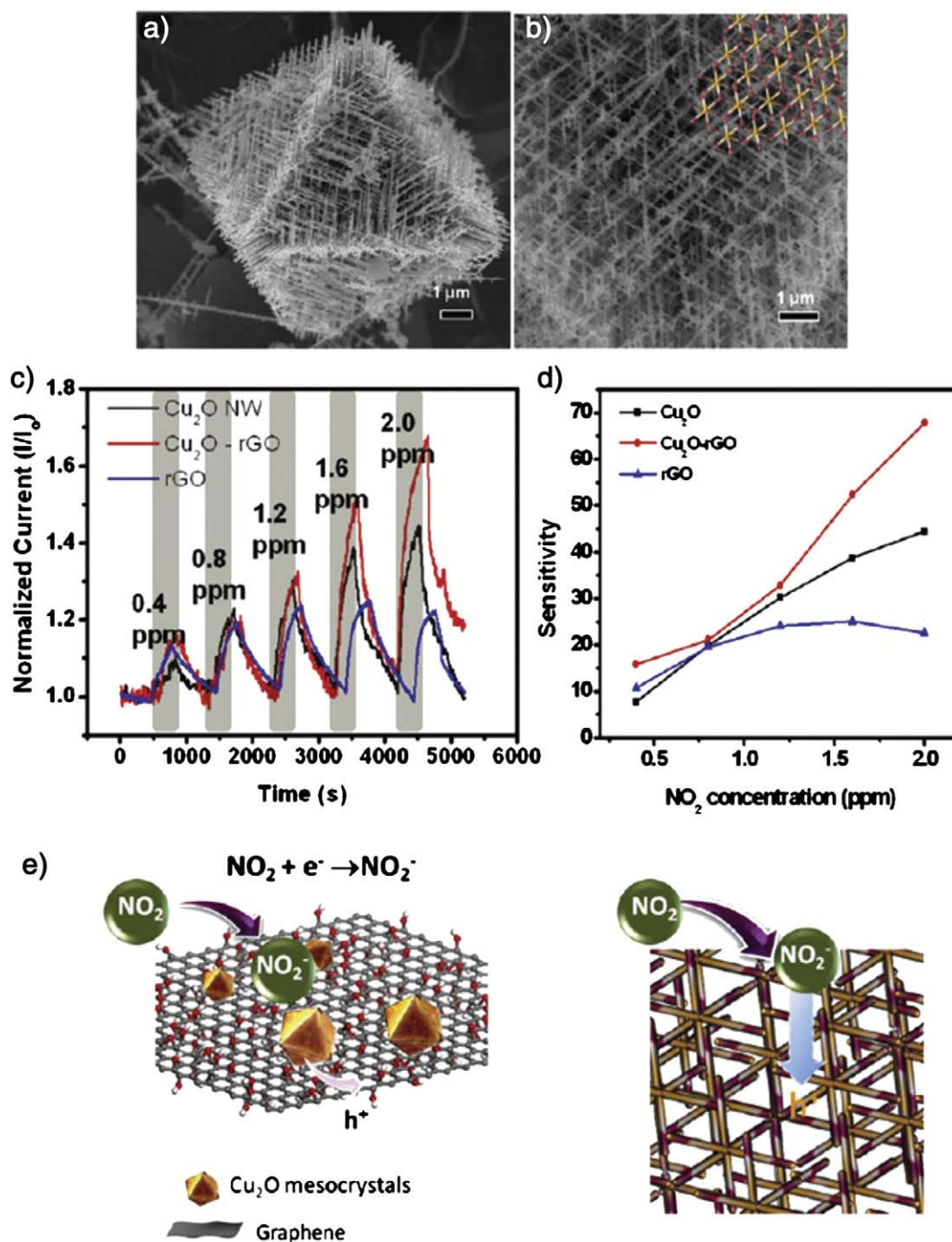


Fig. 3. (a) An octahedral Cu_2O mesocrystal along the [111] view, and (b) interior morphology with overlaid hexapod grid; (c) dynamic response of Cu_2O nanowires (NW), reduced graphene oxide- Cu_2O (rGO), and reduced graphene oxide devices under increasing NO_2 exposure; (d) the sensitivities of the NO_2 sensor for the three devices; (e) scheme illustrating the mechanism of NO_2 sensing of reduced graphene oxide- Cu_2O . From Ref. [33]. Reprinted with permission from ACS.

Semiconductor oxide mesocrystals are promising materials for gas sensor applications. For these applications, high porosity and specific surface areas are again advantageous as well as the specific ordered mesocrystal structure.

Reduced graphene oxide conjugated Cu_2O nanowire mesocrystals were synthesized by non classical crystallization of Cu_2O in the presence of graphene oxide and *o* anisidine under hydrothermal conditions [33]. It is observed that these mesocrystals are comprised of highly anisotropic nanowires as building blocks and possess a distinct octahedral morphology with eight {111} equivalent crystal faces (see Fig. 3).

Reduced graphene oxide conjugated Cu_2O nanowire mesocrystals achieved a high sensitivity toward NO_2 at room temperature owing to high specific surface area and improved conductivity (see Fig. 3), surpassing the performance of standalone systems of Cu_2O nanowire networks and reduced graphene oxide sheets. The reduced graphene oxide conjugated Cu_2O nanowire mesocrystals could have promising applications as ultrasensitive environmental sensors.

A polymer (poly(sodium 4 styrenesulfonate)) mediated route was applied to the synthesis of concave Co_3O_4 octahedral mesocrystals by oriented aggregation of Co_3O_4 primary nanoparticles along their [100] directions [34]. It was found that Co_3O_4 octahedral mesocrystals showed enhanced gas sensing properties of high sensitivity and good response and recovery characteristics by testing the gas sensing performance of the Co_3O_4 mesocrystals with formaldehyde and ethanol as probe analytes. As compared with Co_3O_4 powder, the Co_3O_4 mesocrystals exhibit 1.8 fold and 1.4 fold enhancement in gas responses to 100 ppm of formaldehyde and ethanol, respectively.

Pang et al. observed the inner structure of $\text{W}_{18}\text{O}_{49}$ mesocrystals with a unique mesoporous structure by electron microscopy with the assistance of ultramicrotomy and focused ion beam techniques [35]. It has been shown that at the atomic level, these mesocrystals have long range ordering in one dimension, but only short range ordering in the other two dimensions. The $\text{W}_{18}\text{O}_{49}$ mesocrystals exhibit superior performance toward NO_2 in gas sensing applications compared to nanowire bundles with a comparable surface area and identical compositions. The better performance of the mesocrystals can be attributed to the presence of more oxygen vacancy sites in the unique mesoporous structure.

Porous platelike α Fe_2O_3 mesocrystals were obtained at a low temperature by controlling the self assembly of nanoparticles in the presence of an ionic liquid [Bmim]Cl, which acted as the solvent and the templating reagent [36]. Compared to an Au/ α Fe_2O_3 (Fluka) catalyst, the Au/porous platelike α Fe_2O_3 mesocrystal catalyst displayed a significantly enhanced CO oxidation activity, as a result of a more highly exposed (110) facet in the porous platelike α Fe_2O_3 mesocrystals. Moreover, good repeatability and fast response and recovery times were obtained in an acetone sensitivity test conducted on the α Fe_2O_3 nanoplates, produced via annealing of the porous platelike α Fe_2O_3 mesocrystals at 400 °C, attributed to their plate like morphology and high crystallinity. Furthermore, gas sensing experiments demonstrate that the porous platelike α Fe_2O_3 mesocrystals annealed at a higher temperature exhibit a significantly improved performance compared to the porous platelike α Fe_2O_3 mesocrystals annealed at a lower temperature.

Thin films of copper oxides with controlled crystal phases and morphologies such as CuO, Cu_2O , and $\text{Cu}_2(\text{OH})_3\text{Cl}$ were recently selectively synthesized by using direct or intermediate routes via a microbial mineralization process [37]. Notably, CuO mesocrystalline nanosheets formed a thin film over the whole substrate. The resultant CuO mesocrystal nanosheets showed enhanced properties for the electrochemical detection of dopamine. This study shows the potential applicability of microbial mineralization inspired approaches to thin film coatings.

2.4. Optoelectronic applications

While mesocrystal applications in the fields of photocatalysis, lithium ion batteries, electrodes and gas sensors are the most widely

reported so far, promising mesocrystal applications in optical and optoelectronic devices also exist, although they are still quite rare.

Polymer controlled crystallization has been successfully transferred to functional aromatic organic dyes (3,4,9,10 perylene-tetracarboxylic acid potassium salt (PTCAPS)) modified by the cationic double hydrophilic block copolymer poly(ethylene glycol) *block* branched poly(ethyleneimine) (PEG *b* PEI) [38]. Ultralong hierarchically structured PTCAPS mesocrystalline microbelts with constant width and thickness of each individual belt have been fabricated via an easy room temperature self assembly process (see Fig. 4). The belts are a mesocrystalline assembly of primary nanoparticles with high energy anionic {001} faces stabilized by polymer complexation and show a metallic gloss (Fig. 4) indicative of mobile electrons. Indeed, electrical conductivity measurements performed on a single nanobelt disclose in the electron doped state a remarkably high electronic conductivity and further demonstrate extended, wire like π π interactions along the [020] long axis of the belts. Also, the belts showed fluorescence with different colors depending on the excitation wavelength (see Fig. 4). Together with the very large macroscopic length of the belts and their organic inorganic hybrid nanostructure, this makes these fluorescent organic wires potentially interesting for the field of nano /micro optoelectronics.

A one step refluxing approach was applied for the synthesis of β $\text{Co}(\text{OH})_2$ /brilliant blue G (G250) hybrid microstructures with flower shape composed of mesocrystal nanosheets by the soft templating effect of a CTAB G250 complex through ionic self assembly [39]. This hybrid material with quite high surface area ($95 \text{ m}^2 \text{ g}^{-1}$) exhibits a red shift of the β $\text{Co}(\text{OH})_2$ /G250 absorption peak by 46 nm and an electrochemical catalytic activity for oxygen reduction. This suggests applications in oxygen reduction reactions, photoelectrical applications as well as the application as pigment.

Uniform quasi octahedral CeO_2 mesocrystals could be prepared via particle mediated crystallization involving oriented attachment by a surfactant free non aqueous method using $\text{Ce}(\text{NO}_3)_3$ and octanol as the reactants at 150 °C [40]. Optical characterization revealed a strong quantum confinement, characteristic of the small size of the primary nanocrystals. The thermal stability and UV vis study reveal that the CeO_2 mesocrystal has potential for high temperature applications and optical apparatus applications.

The pre orientation of inorganic colloidal nanoparticles into a mineral liquid crystal is a favorable starting point to enable and study the formation of a structural variety of mesocrystals. Vanadium pentoxide mesocrystals were formed via a liquid crystalline precursor phase using this strategy and three different approaches [41]. Salt could be added to decrease the Debye length of the electric double layer stabilizing the V_2O_5 sol and an ordered agglomeration took place, leading to pillow like, three dimensional, porous superstructures. Salt addition is presumably the least controlled way to promote particle alignment and mesocrystallization. Using high centrifugal fields, long extended fibers formed, which were further compacted toward partly highly organized three dimensional fiber structures. As judged by the very good packing structure and density on the mesoscale, this was evaluated to be the kinetically most controlled and most gentle approach toward mesocrystal formation from tactoids. The third route toward mesocrystals employed a surface active polymer, which adsorbs and stabilizes the {020} faces of the nanoparticles, which form the tactoid thus leading to ordered nanoparticle assembly. The data illustrated the superiority of the polymer approach, as compared to salt destabilization but none of the three reported methods led to completely ordered mesocrystals. Vanadium pentoxide mesocrystals combining high crystallinity with high porosity and larger specific surface area might be useful as a catalyst and also for optoelectronic applications because the material shows electrochromism.

A solvothermal method was also applied for the fabrication of flower like $\text{W}_{18}\text{O}_{49}$ mesocrystals built from individual single crystalline nanowires [42]. The mesocrystals showed stable and reversible electrochromic

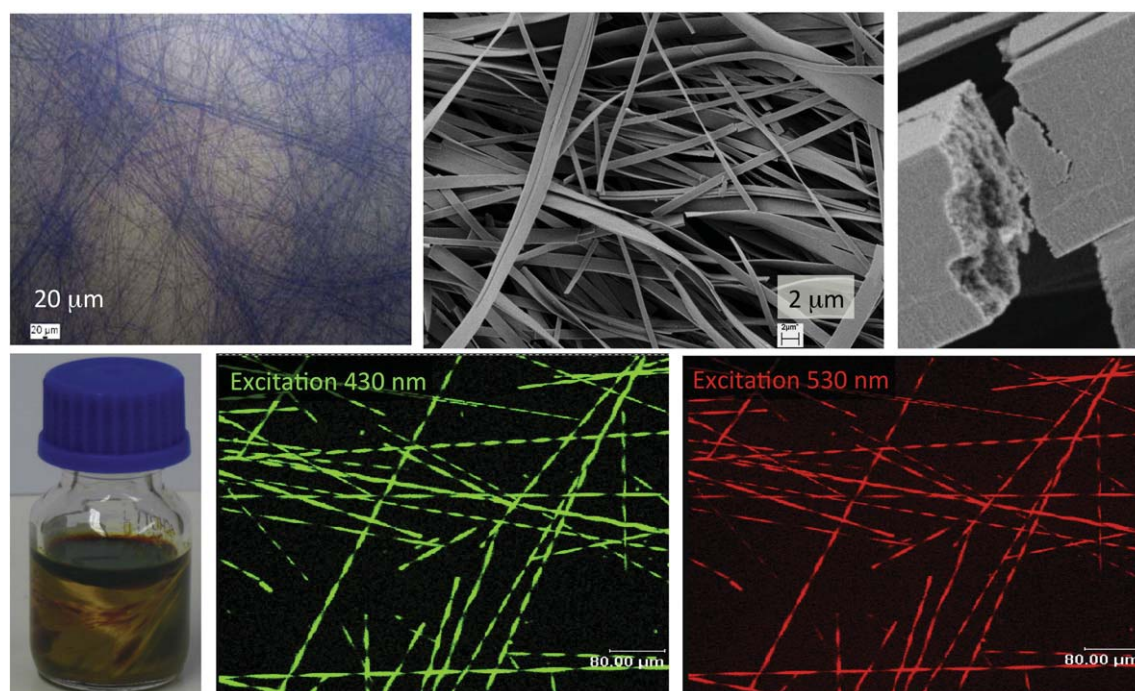


Fig. 4. Ultralong hierarchically structured PTCAPS mesocrystalline microbelts. Upper row: left: light microscopy image of the microbelts in solution, center: SEM image of the microbelts, right: SEM image of fracture surface of a mesocrystalline microbelt showing the granular nanoparticle surface. Lower row: left: photo of the microbelt preparation showing the metallic gloss of the sample, center and right: fluorescence micrograph of the same area of the microbelts in solution excited at two different wavelengths. Figure reproduced from Ref. [38^{**}]. Reprinted with permission from ACS.

performance with high color contrast based on the analyses of cyclic voltammetric curves and UV vis transmittance spectra. This was attributed to their hierarchical architecture, special tunnel structure, and non stoichiometric characteristics. Such electrochromic mesocrystals are promising for potential applications in smart windows.

2.5. Biomedical applications

Mesocrystals were first synthesized by living organisms in the process of biomineralization [8]. Since biominerals are essential components of the human body (bones and teeth), they have a huge impact for (bio)medicine. In view of this importance and the fact that mesocrystals are obviously evolutionary advantageous to fulfill various important functions of a living organism like mechanical strength in the case of bones, it is most remarkable how rare reports on the application of mesocrystals in the biomedical field are. We can therefore currently only refer to a single report.

Yu et al. reported the synthesis of hollow spindle like YF_3 , $\text{YF}_3:\text{Ce}^{3+}$ and $\text{YF}_3:\text{Ce}^{3+}/\text{Ln}^{3+}$ ($\text{Ln} = \text{Tb}, \text{Eu}$) mesocrystals by a solvothermal process using yttrium nitrate and NH_4F as precursors [43^{*}]. The formation of hollow spindle like YF_3 could be ascribed to a non classical crystallization process by means of a particle based reaction route in ethanol. The fluorine sources were found to have a remarkable effect on the morphologies and crystalline phases of the final products. Ce^{3+} is an efficient sensitizer for Ln^{3+} in the spindle like YF_3 mesocrystals. $\text{Ce}^{3+}/\text{Ln}^{3+}$ co doped YF_3 mesocrystals displayed remarkable fluorescence enhancement. The cytotoxicity study revealed that these YF_3 based nanocrystals are biocompatible for applications such as cellular imaging.

2.6. Other applications

Although most mesocrystal applications so far are in the photocatalysis, battery applications or sensor sector, mesocrystals have the potential to be useful in many more areas. For example, mechanically improved materials could much benefit from the mesocrystal design

as demonstrated by various biominerals like the sea urchin spine [9^{**}] and others [8]. Recent work has shown how mesocrystalline architecture and hierarchy can lead to the remarkable structures and properties of biominerals. One example is an adult sea urchin spine, which is a hierarchical mesocrystalline structure of Mg calcite nanocrystals. These nanocrystals are covered by amorphous layers likely as a barrier for the propagation of cracks, which otherwise proceed very easily along crystal cleavage planes, to improve the mechanical material properties [9^{**}]. This is evident in the chonchoidal fracture instead of the flat cleavage plane of a single crystal. A structural model of the adult sea urchin spine was used to explain the observed mechanical properties. Nature obviously demonstrates how mesocrystals can be used to form composite materials with remarkable and highly controllable structures and properties. This has enormous potential for the translation of similar design strategies for the fabrication of synthetic functional (biomedical) materials.

Tremel et al. took inspiration from such natural materials and developed the formation of needle like calcite mesocrystals that resemble naturally occurring *Sycon* sp. *monoaxons* by using the self assembly properties of silicatein α [44^{**},45]. The self assembled spicules with 10 to 300 μm in length and 5 to 10 μm in diameter are composed of aligned calcite nanocrystals with silicatein α occluded in the domain boundaries. The spicules are initially amorphous but transform into calcite within months, exhibiting unusual growth along [100]. The Young's modulus of 14 GPa for synthetic spicules is at least as high as that for natural spicules. Synthetic spicules sustain a fracture stress at least three times higher than that of natural spicules, without any sign of brittle fracture. This results in the possibility to bend the spicule by much more than 90° (see Fig. 5). Interestingly, the presence of only 10 to 16% organic components in combination with calcite nanocrystals accounts for these remarkable mechanical properties. In addition, the spicules exhibit waveguiding properties even when they are bent. This shows in an impressive way, which outstanding mechanical properties are possible with an organic inorganic mesocrystal design.

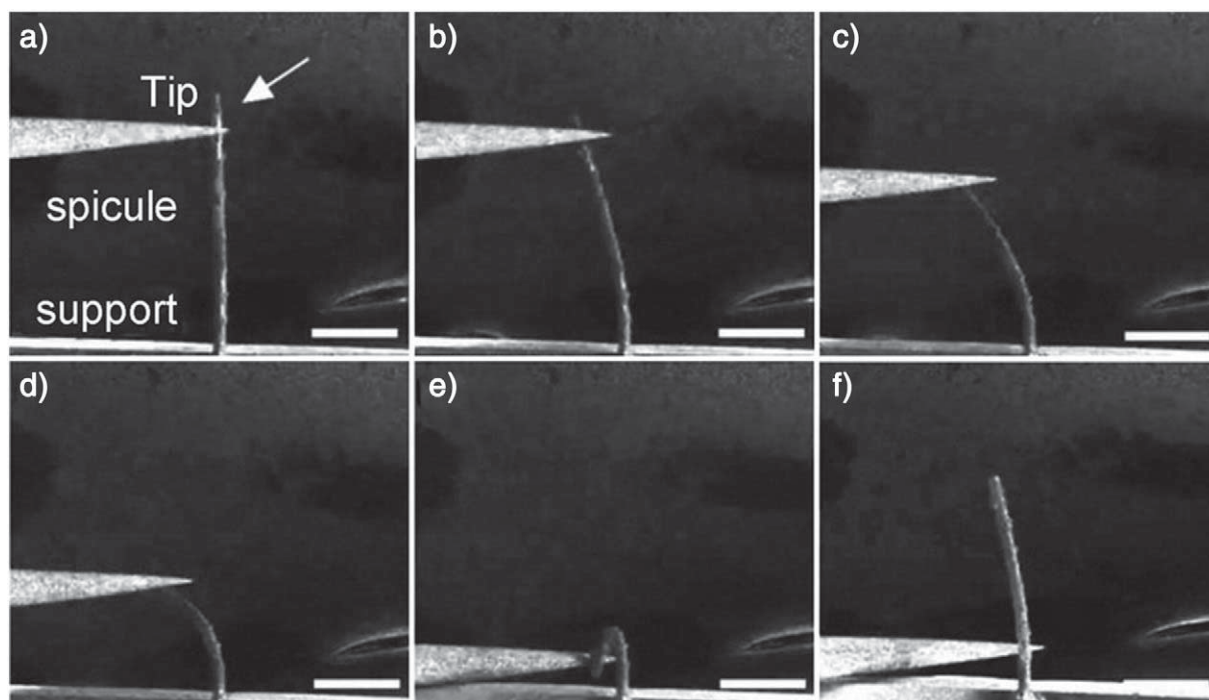


Fig. 5. Time series (a–f) of SEM images illustrating a bending test with a micromanipulator. The synthetic calcitic spicule does not fracture even under extreme deflection, and shows a small plastic component upon release (f). The scale bar is 50 μm . From Ref. [44^{*}]. Reprinted with permission from AAAS.

Not only mechanical but also optical properties of materials can be improved by a mesocrystalline structure like antireflective properties in the following example. Qi's group applied a hydrothermal method for the growth of mesocrystalline rutile TiO_2 nanorod arrays on Ti substrates using tetrabutyl titanate and HCl at 150 $^\circ\text{C}$ for 20 h [46^{*}]. It was found that these ordered rutile mesocrystals displayed excellent quasi omnidirectional antireflective properties. Specular reflectance spectra indicated that light reflection with $<0.5\%$ in the visible region and $<2\%$ in the near infrared region was obtained at an incident angle of 45° . This is by far better than the reference of the Ti foil, which exhibited 10–20% reflection for the visible region and 20–40% for the near infrared region ranging from 800 to 2400 nm. The amazing quasi omnidirectional antireflective properties were suggested to be the result of the hierarchical tips on rod structure of the mesocrystalline nanorods. It is expected that these rutile mesocrystalline nanorod arrays have further application potential including solar cells, displays, and chemical sensors.

Often, it is problematic to coat crystalline thin films onto a surface without cracks. If the coating is single crystalline, cracks are unavoidable due to volume shrinkage upon crystallization. This problem could be solved with a mesocrystal design by a simple evaporation of a polymer induced liquid precursor phase formed from DL lysine·HCl, poly(acrylic acid), water, and EtOH after depositing droplets of the quaternary dispersions onto hydrophilic cover slips [47^{*}]. The thin film formation follows a multistage crystallization process including the formation of a polymer induced liquid precursor phase, the formation of intermediate spherulitic thin films, and the recrystallization of mosaic mesocrystal thin films. The resulting mesocrystalline thin films are porous in nature, and the nanoparticles can rearrange slightly to release the tension between neighboring domains. This avoids crack formation, while the mesocrystal structure gives the film properties of the single crystal. Such single crystal like coatings are interesting for a variety of applications, which exploit the properties of single crystals.

The same system can be used to introduce hierarchy to the mesocrystalline thin films by a simple variation of the experimental

conditions. If the polymer induced liquid precursor phase is allowed to crystallize instead of immediate evaporation, hierarchical mesocrystalline DL lysine·HCl poly(acrylic acid) hybrid thin films with at least five hierarchy levels are formed [48^{*}]. The synthesis procedure could be extended to similar DL lysine thin films, which represent a hierarchical mesocrystalline chiral thin film. Such porous films could be applied in chiral separation or as chiral catalysts. It remains to be shown how general the synthesis concept of mesocrystalline thin films via polymer induced liquid precursor phases is but if it works, it yields highly attractive porous mesocrystalline crack free thin film coatings via a simple evaporation route.

3. Conclusions

A considerable amount of work was dedicated to the application potential of mesocrystals in the last three years. So far, the main applications of mesocrystals are in the areas of photocatalysis, lithium ion batteries, electrodes and sensors. These applications take advantage of the porosity and high surface area of mesocrystals as well as their high crystallinity and orientation of their subunits and result in the observed improved performance of the mesocrystals. In many examples, mesocrystals outperform existing materials for the same application and in some cases, really outstanding properties could be achieved like for example the extremely high capacity of SnO_2 mesocrystal electrode based batteries [29^{*}] almost reaching the theoretical value or the extreme bending strength of calcite mesocrystalline spicules [44^{*}]. A large variety of synthesis approaches including hydrothermal synthesis, topochemical transformations or particle mediated non classical crystallization was reported for the synthesis of functional mesocrystals. Especially hydrothermal methods seem to be very suitable for the synthesis of functional mesocrystals. However, since the basic formation mechanisms of mesocrystals are still poorly understood, we believe that there is still much room to improve the syntheses of mesocrystals as well as their structure. It will also be mandatory to check thoroughly, if the synthesized structures are indeed mesocrystals, meaning

they consist of crystalline nanoparticles with mutual orientation. A number of studies can be found in the literature, which report on mesocrystal properties without a proof that the investigated structures are indeed mesocrystals. Therefore, to reveal the real application potential of mesocrystals, it will be vital to prove the mesocrystal structure and correlate it to its properties. This will facilitate establishing structure-property relationships and is a first step toward the rational design of these very interesting systems.

4. Future perspectives

The current increased research effort toward mesocrystals with application potential will without doubt lead to the improvement of existing mesocrystal applications as well as new applications. Since the current lack in understanding of mesocrystal formation mechanisms hampers a rational design of mesocrystals, a real explosion of mesocrystal applications can be expected once at least several mesocrystal formation mechanisms are understood theoretically. Currently, this seems out of reach but the remarkable progress in analytical techniques—most importantly liquid cell (HR)TEM [49]—will allow one to observe mesocrystal formation in real time, which will greatly enhance our understanding of how these fascinating structures are built. Also an increasing number of detailed structural investigations of mesocrystals [50], will further contribute toward a deeper understanding.

Besides the abovementioned research efforts toward the long term goal of rational mesocrystal design for specific applications, it is believed that very soon, the application range for mesocrystals will be significantly expanded. The mesocrystal structure offers a large variety of combinations with a second type of material (for example organic-inorganic hybrid mesocrystals), which has the potential to lead to emergent material properties. Mesocrystals are promising candidates for applications in various fields such as catalysis, magnetic materials, drug delivery, mechanically optimized materials, electrochemical materials and biomedical materials to give a few examples besides photocatalysis, lithium ion battery, electrode and sensor applications. Especially for biomedical applications, a huge increase of mesocrystal applications can be expected in view of the fact, that nature is also using mesocrystalline structures for the formation of biominerals like bone.

But apart from the abovementioned macroscopic mesocrystal applications it is an exciting future perspective to consider a mesocrystal as a nanodevice in itself, which could exploit the order of the nanoparticle units in a mesocrystal. It is expected that mesocrystals will find applications as nanodevices. For this, controlled deposition of mesocrystals on a surface could be helpful like the TiO₂ nanorod arrays reported by Qi et al. [46], which could then for example be interspaced by a conductor like a conducting polymer. But the real potential as a nanodevice is seen in binary mesocrystals, similar to the binary superlattices [51], which allow for the combination of different nanoparticles toward new materials like metamaterials. One example is the combination of gold nanoparticles with quantum dots, which will fluoresce at the plasmon absorbance to compensate for the energy loss due to absorption. There are so many application possibilities one can think of, which could take advantage of the unique properties of the mesocrystal structure, that further mesocrystal materials with outstanding properties are expected in many application areas. It will be most exciting to see what the future will bring in this area.

Acknowledgments

Financial support from the Fundamental Research Funds for the Central Universities (no. JC2013 3) and the Beijing Nova Program (Z121103002512030) is gratefully acknowledged.

References and recommended reading^{*,**}

- [1] Cölfen H, Antonietti M. Mesocrystals: inorganic superstructures made by highly parallel crystallization and controlled alignment. *Angew Chem Int Ed* 2005;44:5576–91.
- [2] Niederberger M, Cölfen H. Oriented attachment and mesocrystals: non-classical crystallization mechanisms based on nanoparticle assembly. *Phys Chem Chem Phys* 2006;8:3271–87.
- [3*] Cölfen H, Antonietti M. Mesocrystals and non classical crystallization. New York: Wiley; 2008. The first textbook in the mesocrystal field. This book introduces the concept, mechanism, analysis, and properties of mesocrystals, and discusses the difference between classical crystallization and nonclassical crystallization.
- [4] Zhou L, O'Brien P. Mesocrystals: a new class of solid materials. *Small* 2008;4:1566–74.
- [5*] Song RQ, Cölfen H. Mesocrystals—ordered nanoparticle superstructures. *Adv Mater* 2010;22:1301–30. Recent overview about mesocrystals and four basic mesocrystal formation mechanisms.
- [6] Fang JX, Ding BJ, Gleiter H. Mesocrystals: syntheses in metals and applications. *Chem Soc Rev* 2011;40:5347–60.
- [7] Zhou L, O'Brien P. Mesocrystals-Properties and applications. *J Phys Chem Lett* 2012;3:620–8.
- [8] Oaki Y, Kotachi A, Miura T, Imai H. Bridged nanocrystals in biominerals and their biomimetics: classical yet modern crystal growth on the nanoscale. *Adv Funct Mater* 2006;16:1633–9.
- [9**] Seto J, Ma YR, Davis SA, Meldrum F, Gourrier A, Kim YY, et al. Structure-property relationships of a biological mesocrystal in the adult sea urchin spine. *PNAS* 2012;109:3699–704. This study is among the most detailed structural characterizations of a biological mesocrystal allowing much insight into structure and the relation to the material properties. A rich source of inspiration.
- [10**] Tartaj P, Amarilla JM. Multifunctional response of anatase nanostructures based on 25 nm mesocrystal-like porous assemblies. *Adv Mater* 2011;23:4904–7. nm porous anatase mesocrystals with good photodegradation ability, electrochemical performance, and good capability for enzyme immobilization synthesized by the methodology of thermally driven self-assembly of inverse nanomicelles and seeded assisted hydrolysis of precursors.
- [11] Tartaj P. Sub-100 nm TiO₂ mesocrystalline assemblies with mesopores: preparation, characterization, enzyme immobilization and photocatalytic properties. *Chem Commun* 2011;47:256–8.
- [12*] Zhang AY, Long LL, Li WW, Wang WK, Yu HQ. Hexagonal microrods of anatase tetragonal TiO₂: self-directed growth and superior photocatalytic performance. *Chem Commun* 2013;49:6075–7. mesocrystalline hexagonal microrods with a superior photocatalytic capacity due to their high crystallinity, large porosity and oriented subunit alignment as well as exposed high-energy 001 facets.
- [13] Zhou L, Chen J, Ji C, Zhou L, O'Brien P. A facile solid phase reaction to prepare TiO₂ mesocrystals with exposed 001 facets and high photocatalytic activity. *CrystEngComm* 2013;15:5012–5.
- [14] Da Silva RO, Goncalves RH, Stroppa DG, Ramirez AJ, Leite ER. Synthesis of recrystallized anatase TiO₂ mesocrystals with Wulff shape assisted by oriented attachment. *Nanoscale* 2011;3:1910–6.
- [15] Chen QF, Chen CC, Ji HW, Ma WH, Zhao JC. Surfactant-additive-free synthesis of 3D anatase TiO₂ hierarchical architectures with enhanced photocatalytic activity. *RSC Adv* 2013;3:17559–66.
- [16**] Bian ZF, Tachikawa T, Kim W, Choi W, Majima T. Superior electron transport and photocatalytic abilities of metal-nanoparticle-loaded TiO₂ superstructures. *J Phys Chem C* 2012;116:25444–53. Novel nanocomposites containing plate-like anatase TiO₂ mesocrystal superstructures and noble metal (Au, Pt) nanoparticles, which greatly improve the photogenerated charge separation efficiency by metal nanoparticles preferentially deposited on the edge of the TiO₂ mesocrystals.
- [17*] Yang XF, Qin JL, Li Y, Zhang RX, Tang H. Graphene-spindle shaped TiO₂ mesocrystal composites: facile synthesis and enhanced visible light photocatalytic performance. *J Hazard Mater* 2013;261:342–50. Graphene-TiO₂ spindle shaped mesocrystal composites with high photocatalytic activity via a facile template-free process based on the combination of sol-gel and solvothermal methods.
- [18] Liu YQ, Zhang Y, Wang J. From NH₄TiOF₃ nanoparticles to NH₄TiOF₃ mesocrystals: steric hindrance versus hydrophobic attraction of F127 molecules. *CrystEngComm* 2013;15:791–801.
- [19*] Dong JY, Lin WH, Hsu YJ, Wong DSH, Lu SY. Ultrafast formation of ZnO mesocrystals with excellent photocatalytic activities by a facile Tris-assisted antisolvent process. *CrystEngComm* 2011;13:6218–22. A room temperature ionic liquid based process was used for the ultrafast formation of ZnO mesocrystals with high specific surface areas and excellent photocatalytic activity towards photodegradation of methylene blue.
- [20] Yang YQ, Yang YQ, Wu HX, Guo SW. Control of the formation of rod-like ZnO mesocrystals and their photocatalytic properties. *CrystEngComm* 2013;15:2608–15.
- [21*] Sun SD, Zhang XZ, Zhang J, Wang LQ, Song XP, Yang ZM. Surfactant-free CuO mesocrystals with controllable dimensions: green ordered-aggregation-driven synthesis, formation mechanism and their photochemical performances. *CrystEngComm* 2013;15:867–77.

* Of special interest.

** Of outstanding interest.

- The ordered aggregation driven growth from surfactant-free one-dimensional (1D) CuO nanocrystals into dimension-controlled mesostructures (three-dimensional (3D) mesocrystalline spindles and two-dimensional (2D) mesocrystal plates) with a high adsorption and photocatalytic degradation of Rhodamine B by an additive-free complex-precursor solution route.
- [22••] Sun JX, Chen G, Pei J, Jin RC, Wang Q, Guang XY. A simple approach to strontium sodium tantalite mesocrystals with ultra-high photocatalytic properties for water splitting. *J Mater Chem* 2012;22:5609–14. Strontium sodium tantalite mesocrystal with outstanding photocatalytic performance built from nanocubes (20–60 nm) via a non-classical crystallization process by a simple molten salt process.
- [23] Kuang Q, Yang SH. Template synthesis of single-crystal-like porous SrTiO₃ nanocube assemblies and their enhanced photocatalytic hydrogen evolution. *ACS Appl Mater Interfaces* 2013;5:3683–90.
- [24••] Hong ZS, Wei MD, Lan TB, Jiang LL, Cao GZ. Additive-free synthesis of unique TiO₂ mesocrystals with enhanced lithium-ion intercalation properties. *Energy Environ Sci* 2012;5:5408–13. A low-temperature additive-free synthetic route for the fabrication of unique nanorod-like mesocrystals with large reversible charge-discharge capacity and excellent cycling stability through homoepitaxial aggregation of ultrathin rutile TiO₂ nanowires via face-to-face oriented attachment, accompanied and promoted by a simultaneous phase transformation from precursor hydrogen titanate to rutile TiO₂.
- [25•] Hong ZS, Wei MD, Lan TB, Cao GZ. Self-assembled nanoporous rutile TiO₂ mesocrystals with tunable morphologies for high rate lithium-ion batteries. *Nano Energy* 2012;1:466–71. Wulff-shaped and nanorod-like nanoporous mesocrystals with a large reversible charge-discharge capacity, excellent cycling stability and high rate performance constructed by ultrathin rutile TiO₂ nanowires through homoepitaxial self-assembly of nanocrystallites with the assistance of sodium dodecyl benzene sulfonate.
- [26] Hong ZS, Xu YX, Liu YB, Wei MD. Unique ordered TiO₂ superstructures with tunable morphology and crystalline phase for improved lithium storage properties. *Chem Eur J* 2012;18:10753–60.
- [27•] Ye JF, Liu W, Cai JG, Chen S, Zhao XW, Zhou HH, et al. Nanoporous anatase TiO₂ mesocrystals: additive-free synthesis, remarkable crystalline-phase stability, and improved lithium insertion behavior. *J Am Chem Soc* 2011;133:933–40. Spindle-shaped nanoporous anatase TiO₂ mesocrystals with remarkable crystalline-phase stability and improved performance as anode materials for lithium ion batteries under the assistance of acetic acid molecules.
- [28] Hong ZS, Wei MD. Layered titanate nanostructures and their derivatives as negative electrode materials for lithium-ion batteries. *J Mater Chem A* 2013;1:4403–14.
- [29••] Chen S, Wang M, Ye JF, Cai JG, Ma YR, Zhou HH, et al. Kinetics-controlled growth of aligned mesocrystalline SnO₂ nanorod arrays for lithium-ion batteries with superior rate performance. *Nano Res* 2013;6:243–52. Aligned nanorod arrays of [001]-oriented mesocrystalline SnO₂ with four 110 lateral facets and a very high reversible capacity of 720 mA h g⁻¹ synthesized on Ti foil in a ternary solvent system comprising acetic acid, ethanol, and water via a kinetically controlled growth strategy.
- [30•] Xu MW, Wang F, Ding BJ, Song XP, Fang JX. Electrochemical synthesis of leaf-like CuO mesocrystals and their lithium storage properties. *RSC Adv* 2012;2:2240–3. Electrochemical synthesis of leaf-like CuO mesocrystals via the oriented attachment mechanism with high specific capacity and good cycle performance.
- [31•] Hou LR, Yuan CZ, Yang L, Shen LF, Zhang F, Zhang XG. Biomolecule-assisted hydrothermal approach towards synthesis of ultra-thin nanoporous a-Co(OH)₂ mesocrystal nanosheets for electrochemical capacitors. *CrystEngComm* 2011;13:6130–5. Two dimensional ultra-thin a-Co(OH)₂ mesocrystal nanosheets with good electrical conductivity by a biomolecule-assisted hydrothermal strategy for electrochemical capacitors and Li-ion batteries.
- [32] Dang F, Hoshino T, Oaki Y, Hosono E, Zhou H, Imai H. Synthesis of Li–Mn–O mesocrystals with controlled crystal phases through topotactic transformation of MnCO₃. *Nanoscale* 2013;5:2352–7.
- [33•] Deng SZ, Tjoa V, Fan HM, Tan HR, Sayle DC, Olivo M, et al. Reduced graphene oxide conjugated Cu₂O nanowire mesocrystals for high-performance NO₂ gas sensor. *J Am Chem Soc* 2012;134:4905–17. Reduced graphene oxide-conjugated Cu₂O nanowire mesocrystals obtained by nonclassical crystallization of Cu₂O in the presence of graphene oxide and *o*-anisidine under hydrothermal conditions with a high sensitivity towards NO₂ detection at room temperature owing to high specific surface area and improved conductivity.
- [34] Liu YJ, Zhu GX, Ge BL, Zhou H, Yuan AH, Shen XP. Concave Co₃O₄ octahedral mesocrystal: polymer-mediated synthesis and sensing properties. *CrystEngComm* 2012;14:6264–70.
- [35] Wang D, Sun JB, Cao X, Zhu YH, Wang QX, Wang GC, et al. High-performance gas sensing achieved by mesoporous tungsten oxide mesocrystals with increased oxygen vacancies. *J Mater Chem A* 2013;1:8653–7.
- [36] Ma JM, Teo J, Mei L, Zhong ZY, Li QH, Wang TH, et al. Porous platelike hematite mesocrystals: synthesis, catalytic and gas-sensing applications. *J Mater Chem* 2012;22:11694–700.
- [37] Ikeda T, Oaki Y, Imai H. Thin films that consist of CuO mesocrystal nanosheets: an application of microbial-mineralization-inspired approaches to thin-film formation. *Chem Asian J* 2013;8:2064–9.
- [38••] Huang MH, Schilde U, Kumke M, Antonietti M, Cölfen H. Polymer-induced self-assembly of small organic molecules into ultralong microbelts with electronic conductivity. *J Am Chem Soc* 2010;132:3700–7. Ultralong hierarchically structured mesocrystalline microbelts with constant width and thickness of each individual belt via an easy room temperature self-assembly process. The belts show multicolour fluorescence and high conductivity.
- [39•] Cong HP, Ren XC, Yao HB, Wang P, Cölfen H, Yu SH. Synthesis and optical properties of mesoporous β-Co(OH)₂/brilliant blue G (G250) hybrid hierarchical structures. *Adv Mater* 2012;24:1309–15. β-Co(OH)₂/brilliant blue G (G250) hybrid microstructures with flower shape composed of mesocrystal nanosheets synthesized exploiting the soft-templating effect of a CTAB-G250 complex through ionic self-assembly via a one-step refluxing approach.
- [40] Wang XD, Ma Y, Sugunan A, Qin J, Toprak MS, Zhu B, et al. Synthesis of uniform quasi-octahedral CeO₂ mesocrystals via a surfactant-free route. *J Nanopart Res* 2011;13:5879–85.
- [41•] Lausser C, Cölfen H, Antonietti M. Mesocrystals of vanadium pentoxide: a comparative evaluation of three different pathways of mesocrystal synthesis from tactosol precursors. *ACS Nano* 2011;5:107–14. Vanadium pentoxide mesocrystals synthesized via a liquid crystalline precursor phase by three different approaches.
- [42] Sun SB, Chang XT, Liu T, Lu YJ, Wang YY. Solvothermal synthesis of tungsten oxide mesocrystals and their electrochromic performance. *Mater Lett* 2013;105:54–7.
- [43•] Zhong SL, Lu Y, Gao MR, Liu SJ, Peng J, Zhang LC, et al. Monodisperse mesocrystals of YF₃ and Ce³⁺/Ln³⁺ (Ln = Tb, Eu) co-activated YF₃: shape control synthesis, luminescent properties, and biocompatibility. *Chem Eur J* 2012;18:5222–31. Hollow spindle-like YF₃, YF₃:Ce³⁺ and YF₃:Ce³⁺/Ln³⁺ (Ln = Tb, Eu) mesocrystals obtained using a nonclassical crystallization process by means of a particle-based reaction route in ethanol, display remarkable fluorescence enhancement.
- [44••] Natalio F, Corrales TP, Panthöfer M, Schollmeyer D, Lieberwirth I, Müller WEG, et al. Flexible minerals: self-assembled calcite spicules with extreme bending strength. *Science* 2013;339:1298–302. Needle-like calcite mesocrystals with remarkable mechanical properties that resemble naturally occurring *Sycon* sp. *monoaxons* by using the self-assembly properties of silicatein-α.
- [45] Gebauer D. Bio-inspired materials science at its best-flexible mesocrystals of calcite. *Angew Chem Int Ed* 2013;52:8208–9.
- [46•] Cai JG, Ye JF, Chen SY, Zhao XW, Zhang DY, Chen S, et al. Self-cleaning, broadband and quasi-omnidirectional antireflective structures based on mesocrystalline rutile TiO₂ nanorod arrays. *Energy Environ Sci* 2012;5:7575–81. Mesocrystalline rutile TiO₂ nanorod arrays with high chemical and thermal stability, self-cleaning, excellent broadband, and quasi-omnidirectional antireflective structures by a hydrothermal synthesis directly on Ti foils.
- [47•] Jiang Y, Gong HF, Grzywa M, Volkmer D, Gower L, Cölfen H. Microdomain transformations in mosaic mesocrystal thin films. *Adv Funct Mater* 2013;23:1547–55. Crack free mesocrystalline films by simple evaporation of a polymer-induced liquid-precursor phase from DL-lysine·HCl, poly(acrylic acid), water, and EtOH after depositing droplets of the quaternary dispersions onto hydrophilic cover slips.
- [48•] Jiang Y, Gong HF, Volkmer D, Gower L, Cölfen H. Preparation of hierarchical mesocrystalline DL-lysine·HCl-poly(acrylic acid) hybrid thin films. *Adv Mater* 2011;23:3548–52. Hierarchical mesocrystalline DL-lysine·HCl-poly(acrylic acid) hybrid thin films with at five hierarchy levels via polymer induced liquid precursor phases.
- [49] Li DS, Nielsen MH, Lee JRI, Frandsen C, Banfield JF, De Yoreo JJ. Direction-specific interactions control crystal growth by oriented attachment. *Science* 2012;336:1014–8.
- [50] Simon P, Rosseeva E, Baburin IA, Liebscher L, Hickey SG, Cardoso-Gil R, et al. PbS-organic mesocrystals: the relationship between nanocrystal orientation and superlattice array. *Angew Chem Int Ed* 2012;51:10776–81.
- [51] Shevchenko EV, Talapin DV, Kotov NA, O'Brien S, Murray CB. Structural diversity in binary nanoparticle superlattices. *Nature* 2006;439:55–9.